*Visual Neuroscience* (2015), **32**, e003, 9 pages.
Copyright © Cambridge University Press, 2015 0952-5238/15
doi:10.1017/S0952523814000364

**RESEARCH ARTICLE**

# CaV3.2 KO mice have altered retinal waves but normal direction selectivity

AARON M. HAMBY,[1] JULIANA M. ROSA,[1] CHING-HSIU HSU,[1] AND MARLA B. FELLER[1,2]

[1]Department of Molecular and Cell Biology, University of California, Berkeley, Berkeley, California
[2]Helen Wills Neuroscience Institute, University of California, Berkeley, Berkeley, California

(RECEIVED August 27, 2014; ACCEPTED November 26, 2014)

**Abstract**

Early in development, before the onset of vision, the retina establishes direction-selective responses. During this time period, the retina spontaneously generates bursts of action potentials that propagate across its extent. The precise spatial and temporal properties of these "retinal waves" have been implicated in the formation of retinal projections to the brain. However, their role in the development of direction selective circuits within the retina has not yet been determined. We addressed this issue by combining multielectrode array and cell-attached recordings to examine mice that lack the CaV3.2 subunit of T-type $Ca^{2+}$ channels (CaV3.2 KO) because these mice exhibit disrupted waves during the period that direction selective circuits are established. We found that the spontaneous activity of these mice displays wave-associated bursts of action potentials that are altered from that of control mice: the frequency of these bursts is significantly decreased and the firing rate within each burst is reduced. Moreover, the projection patterns of the retina demonstrate decreased eye-specific segregation in the dorsal lateral geniculate nucleus (dLGN). However, after eye-opening, the direction selective responses of CaV3.2 KO direction selective ganglion cells (DSGCs) are indistinguishable from those of wild-type DSGCs. Our data indicate that although the temporal properties of the action potential bursts associated with retinal waves are important for activity-dependent refining of retinal projections to central targets, they are not critical for establishing direction selectivity in the retina.

**Keywords:** Activity-dependent development, Retinal ganglion cells, Voltage-gated calcium channels, Neurodevelopment

## Introduction

Motion constitutes one of the most salient cues for both vertebrate and invertebrate visual systems. Indeed, multiple distinct circuits at various levels of the visual system are sensitive to the presence of moving objects. Perhaps, the best understood circuit addressing the extraction of motion is that of the ON–OFF direction selective ganglion cell (DSGC) in the mammalian retina. These DSGCs respond strongly to an image moving in the preferred direction and weakly to an image moving in the opposite, or null, direction (Barlow & Hill, 1963). They project to several distinct vision centers in the brain (Huberman et al., 2009; Kay et al., 2011; Rivlin-Etzion et al., 2011) where motion is encoded in postsynaptic targets (Marshel et al., 2012; Piscopo et al., 2013). Though the cellular and synaptic bases of this computation are reasonably well understood, the wiring up of this circuit during development is mostly a mystery (Borst & Euler, 2011; Wei & Feller, 2011).

The development of direction selective circuits does not require visual experience because direction selectivity was already established at eye opening (Chan & Chiao, 2008; Elstrott et al., 2008; Chen et al., 2009; Wei et al., 2011; Chen et al., 2014), though several features of DSGCs are immature at these early ages (Chan & Chiao, 2008, 2013; Chen et al., 2014). However, spontaneous activity may play a role. Prior to the onset of vision, the retina is not silent but rather exhibits highly correlated propagating spontaneous activity termed retinal waves (Galli & Maffei, 1988; Meister et al., 1991; Wong, 1999; Blankenship & Feller, 2010). These waves initiate in random locations and propagate from one cell to another, causing neighboring cells, including DSGCs, to fire correlated bursts of action potentials (Elstrott & Feller, 2010).

In mice, retinal waves are first detected a few days before birth and persist for approximately two weeks after birth, disappearing around the time of eye-opening (Maccione et al., 2014). During this extended developmental period, the retinal circuits undergo significant changes in organization and hence the circuits mediating waves also change. The two most well-studied stages of retinal wave generation are from P1–P10, when waves are mediated by a transient cholinergic circuit (Ford & Feller, 2012) and P11–P14, when waves are mediated by a glutamatergic circuit (Akrouh & Kerschensteiner, 2013; Maccione et al., 2014).

Retinal waves have been implicated in several aspects of visual development. In the retina, they are thought to influence the

Address correspondence to: Marla B. Feller, 142 Life Sciences Additions MSC 3200, University of California at Berkeley, Berkeley, CA 94720-3200. E-mail: mfeller@berkeley.edu



https://doi.org/10.1017/S0952523814000364 Published online by Cambridge University Press

segregation of retinal ganglion cell (RGC) dendrites into distinct synaptic layers that determine their functional output (Sernagor et al., 2001; Tian, 2008). Outside the retina, they are thought to provide the structured activity critical for refining the initially coarse RGC projections to the thalamus and superior colliculus (for reviews, see Huberman et al., 2008; Kirkby et al., 2013). Waves also exhibit a bias in their propagation direction, with more waves propagating toward the nasal direction (Stafford et al., 2009), an effect enhanced in the second postnatal week (Elstrott & Feller, 2010). Hence, the retinal waves provide a robust source of directional information prior to the onset of vision.

Several studies have addressed the role of glutamatergic retinal waves in the development of direction selectivity. These studies are based on intraocular injections of activity blockers and have demonstrated that the direction selective responses are still detected at eye-opening (Sun et al., 2011; Wei et al., 2011). However, with intraocular injections, it is difficult to verify that the activity is being blocked during the entire duration of the manipulation. In addition, these injection studies were based on manipulating nonglutamatergic circuits. Finally, these studies were often based on recordings from individual DSGCs and therefore do not represent a broad sampling across the population.

Here, we use a genetic approach to test whether disrupting glutamatergic retinal waves alters the development of direction selectivity with both targeted recording from genetically identified DSGCs and multielectrode array (MEA) recording from a broader population. A critical component of the network mediating waves and a primary source of the depolarizing input to RGCs is glutamate release from bipolar cells (Akrouh & Kerschensteiner, 2013; Firl et al., 2013). In the adult retina, bipolar cells exhibit unstable membrane potentials and their spontaneous depolarizations are mediated by low-voltage activated T-type calcium channels (Ma & Pan, 2003; Cueni et al., 2009; Puthussery et al., 2014; Sargoy et al., 2014) that are expressed in the subsets of bipolar cells (Pan et al., 2001; Singer & Diamond, 2003) and of ganglion cells (Sargoy et al., 2014). The isoform $\alpha 1_H$ (CaV3.2) of the T-type $Ca^{2+}$ channel (Cueni et al., 2009) localizes to cone bipolar cells. Here, we studied retinal waves and direction selectivity of mice where CaV3.2 is deleted (Chen et al., 2003; Ma & Pan, 2003). We compared the spontaneous activity patterns during development and the direction selective responses in the adult of CaV3.2 knockout (KO) mice to those of their littermate controls.

## Materials and methods

### *Mice*

CaV3.2–/– mice (Chen et al., 2003) were obtained from the Mutant Mouse Regional Resource Center (MMRRC line #9979) and crossed to C57BL/6 in our laboratory. P11–19 CaV3.2 KO mice and littermate controls were maintained on a C57bl/6 background, housed under constant day/night cycles, and provided food and water ad libitum. All animal procedures were approved by the University of California (UC) Berkeley Institutional Animal Care and Use Committees and conformed to the NIH Guide for the Care and Use of Laboratory Animals, the Public Health Service Policy, and the SFN Policy on the Use of Animals in Neuroscience Research. Littermates (CaV3.2+/+ mice) were used as control mice. CaV3.2+/– mice were not included in this study.

### *Multielectrode array recordings of spontaneous activity*

Retinas were removed from CaV3.2 KO mice or CaV3.2+/+ littermates (referred to as control throughout the manuscript) at P11–12 in room light and perfused with oxygenated and pH buffered artificial cerebral spinal fluid (ACSF) and placed ganglion cell side down on a commercial 61 electrode array. Approximately, 1 h recordings of spontaneous activity were made and analyzed as described below.

### *Multielectrode array recordings of visual responses*

Retinas were removed from CaV3.2 KO and CaV3.2+/+ mice P16-P19 in the dark under infrared illumination and placed ganglion cell side down on a commercial 61 electrode array. The presence or absence of direction selective responses was then characterized by stimulating the retina with square pulse drifting gratings presented on a small display placed in the camera port of the microscope. The photoreceptor layer of the isolated piece of retina will be stimulated from above with an optically reduced image of a OLED monitor focused with a microscope objective, centered on the array, and refreshing at 120 Hz (gray screen intensity = 1623 equivalent photons/$\mu m^2$/s at 491 nm). For most experiments, the retina was stimulated with five repetitions of full-field square wave gratings moving in one of 12 randomly interleaved directions, with each presentation lasting 10 s, followed by 3 s of gray screen (800 $\mu$m/period, 1.066 s/period, velocity = 25 deg/s for the adult mouse). In some recordings, full-field sinusoidal gratings may be used (400 $\mu$m/period, 0.533 s/period, velocity = 25 deg/s for the adult mouse).

### *Spike-sorting*

The voltage trace recorded on each electrode was sampled at 20 kHz and stored for offline analysis. Spikes that cross threshold were sorted according to the principal components of their voltage waveforms on neighboring electrodes. Spikes were first projected into the first five principal component dimensions where an expectation maximization algorithm was used to group spikes into a mixture of Gaussians' model. All spike clusters will be inspected manually in a principal component space. The overall direction selective response was characterized in each direction by computing the vector sum of these responses for each cell.

A direction selective index was then calculated for each cell, given by the following formula: D.S.I. = (pref – null)/(pref + null) where pref is the average response in the preferred direction, defined as the stimulus direction closest to the vector sum of all responses, and null is the average response in the stimulus direction 180 deg opposite pref. For a given cell, the width of the tuning curve, which is a measure of the strength of directional tuning and defines the preferred and null axis for each DSGC, is computed by fitting the response curve to a von Mises distribution, given by the following: $R = R_{max} e^{k\cos(x-\mu)} = e^k$, where $R$ is the response to motion in a given stimulus direction $x$ in radians, $R_{max}$ is the maximum response, $\mu$ is the preferred direction in radians, and $k$ is the concentration parameter accounting for tuning width. The tuning width of each cell will be estimated as the full width at half height (fwhh) of the von Mises fit using the following equation: fwhh = $2(\theta - \mu)$, where $\theta = a\cos[\ln(\frac{1}{2}e^k + \frac{1}{2}e^{-k})/k] + \mu$. Calculation of these values allows us to investigate the degree of tuning in nascent DSGCs that have experienced altered activity.

https://doi.org/10.1017/S0952523814000364 Published online by Cambridge University Press

The mean firing rates in the preferred and null directions were computed as previously described (Elstrott et al., 2008). We did not keep track of the orientation of the retinas and therefore the distribution of the preferred directions in visual coordinates was not determined.

### *Data from images: Eye-specific segregation analysis*

Animals were anesthetized with 3.5% isoflurane/2% $O_2$. The eyelid was then opened with fine forceps to expose the eye, and 0.1–1 $\mu$l of Alexa-488 or Alexa-594 conjugated-cholera toxin was injected using a fine glass micropipette with a picospritzer (World Precision Instruments, Sarasota, FL) generating 20 psi, 3 ms long positive pressure. The cholera toxin was then allowed to transport for 24 h, which was sufficient time for a clear labeling of axons and terminals. Brains were removed, immersion fixed in 4% paraformaldehyde (24 h), cryo-protected in 30% sucrose (18 h), and sectioned coronally (100 $\mu$m) on a vibratome.

Images were analyzed as described previously (Torborg & Feller, 2004). Eight-bit tagged image file format images were acquired for Alexa488- or 594-labeled sections of the lateral geniculate nucleus (LGN) with a CCD camera (Optronics, Goleta, CA) attached to an upright microscope (Zeiss Axioscope 2; Thornwood, NY) with a 10x objective (numerical aperture, 0.45). The three sections that contained the largest ipsilateral projection, corresponding to the central third of the LGN, were selected. Background fluorescence was subtracted using a rolling ball filter (ImageJ) and the grayscale was renormalized so that the range of grayscale values was from 0 to 256. IgorPro Software (Wavemetrics, Lake Oswego, OR) was used to perform a segregation analysis. For each pixel, we computed the logarithm of the intensity ratio, $R = \log_{10}(F_I/F_C)$, where $F_I$ is the ipsilateral channel fluorescence intensity and $F_C$ is the contralateral channel fluorescence intensity. We then calculated the variance of the distribution of the *R*-values for each section, which was used to compare the width of the distributions across animals. A higher variance is indicative of a wider distribution of the *R*-values, which is in turn indicative of more contra- and ipsi-dominant pixels, and therefore more segregation.

### *Two-photon targeted recordings from GFP+ RGCs and intracellular fillings*

Filter paper-mounted retinas were placed under the microscope in oxygenated Ames' medium at 32–34 °C. Identification of and recording from GFP+ cells were described in Wei et al. (2010). In short, GFP+ cells were identified using a custom-modified two-photon microscope (Fluoview 300, Olympus America Inc.) tuned to 920 nm to minimize the bleaching of the photoreceptors. The average laser power at the sample was 10 mW. The inner limiting membrane above the targeted cell was dissected with the glass electrode, and loose-patch voltage-clamp recordings (holding voltage set to "OFF") were performed with a new glass electrode (3–5 MΩ) filled with Ames' medium. Data were acquired through an Axopatch 200B (Molecular Devices) and digitized at a sampling rate of 20 kHz.

GFP+ RGCs were first stimulated with five repetitions of a 200 $\mu$m white spot for 2 s to test on and off responses. To test a directional response, we presented three repetitions of drifting square-waves gratings (spatial frequency = 225 mm/cycle, temporal frequency four cycles/s, 30°/s in eight pseudorandomly chosen directions spaced at 45° intervals, with each presentation lasting 3 s followed by 500 ms of gray screen). The directionality of the GFP+ cells was further analyzed as described above.

The dendritic morphology of GFP+ cells was determined by including 0.05 $\mu$M Alexa Fluor 488 (Invitrogen) in the intracellular solution following cell-attached recordings of the spike responses. The dendritic morphology of dye-injected GFP+ RGCs was reconstructed by a two-photon imaging with the laser tuned to 800 nm. Images were acquired at *z* intervals of 0.5 $\mu$m using a 60× objective (Olympus LUMPlanFl/IR 360/0.90W). GFP+ RGC processes were later reconstructed from image stacks with ImageJ.

## Results

### *CaV3.2 KO mice display altered retinal waves*

The T-type channels differ from most other members of the voltage-gated calcium channel (VGCC) family in that they activate at more hyperpolarized membrane potentials and they rapidly inactivate, giving rise to a transient current which contribute to pacemaking and bursting properties of several classes of neurons (Cueni et al., 2009; Cain & Snutch, 2013). There are three identified types of T-type channels, which are categorized both molecularly by their alpha subunit isoform (CaV3.1-3) and physiologically (Perez-Reyes, 2003). Recently, it was determined that the CaV3.2 subtype of T-type current is expressed in the axon terminals of cone bipolar cells (Cui et al., 2012) and therefore we looked at glutamatergic waves in mice lacking the CaV3.2 subunit.

To characterize the firing patterns of CaV3.2 KO (KO) retinas, we used a MEA to record extracellularly from many RGCs simultaneously. From postnatal day 1 (P1) to P10, these waves are mediated by a cholinergic circuit, and from P11 to eye opening, they are mediated by a glutamatergic circuit. In this study, we focused on the glutamatergic circuit since this represents the period when direction selective circuits are established (Wei et al., 2011). We compared the glutamatergic waves by recording from KO mice and their CaV3.2+/+ littermate controls at ages P11–12 ($n$ = 11 KO and 10 control). In control mice, these waves consist of periodic correlated bursts of action potentials separated by interwave intervals with very few action potentials, similar to the firing patterns described previously for wild-type mice (Xu et al., 2010; Blankenship et al., 2011). In KO mice, these waves also display correlated bursts of action potentials, but these bursts last for longer durations and are separated from each other by longer interwave intervals that are completely quiescent (Fig. 1A).

To compare these firing patterns, we quantified several features. First, we computed the correlation index as a function of distance between the cells. Nearest-neighbor correlations are higher for nearby cells than for distant cells, confirming that the firing is due to propagating waves. These correlations are indistinguishable between KO and control retinas (Fig. 1B), indicating that the spatial correlations induced by waves in KO mice are similar to those in control mice. Second, we examined temporal features of the overall firing pattern. We found that the median firing rates (Fig. 1C) were not statistically different (median, Mdn of 0.44 Hz; interquartile range, IQR = 0.27–0.54 in KO *vs*. Mdn of 0.72 Hz; 0.44–1.09 in control $P$ = 0.074), indicating that they exhibit similar levels of firing overall. In contrast, the time spent firing above 10 Hz (PC10), a feature reported to be critical for driving eye-specific segregation of retinogeniculate projections (Torborg et al., 2005), is significantly reduced in KO (Mdn of 0.62%; 0.43–0.90 in KO *vs*. Mdn of 1.43%; 1.01–3.19 in control $P$ = 0.002). Third, we characterized

https://doi.org/10.1017/S0952523814000364 Published online by Cambridge University Press

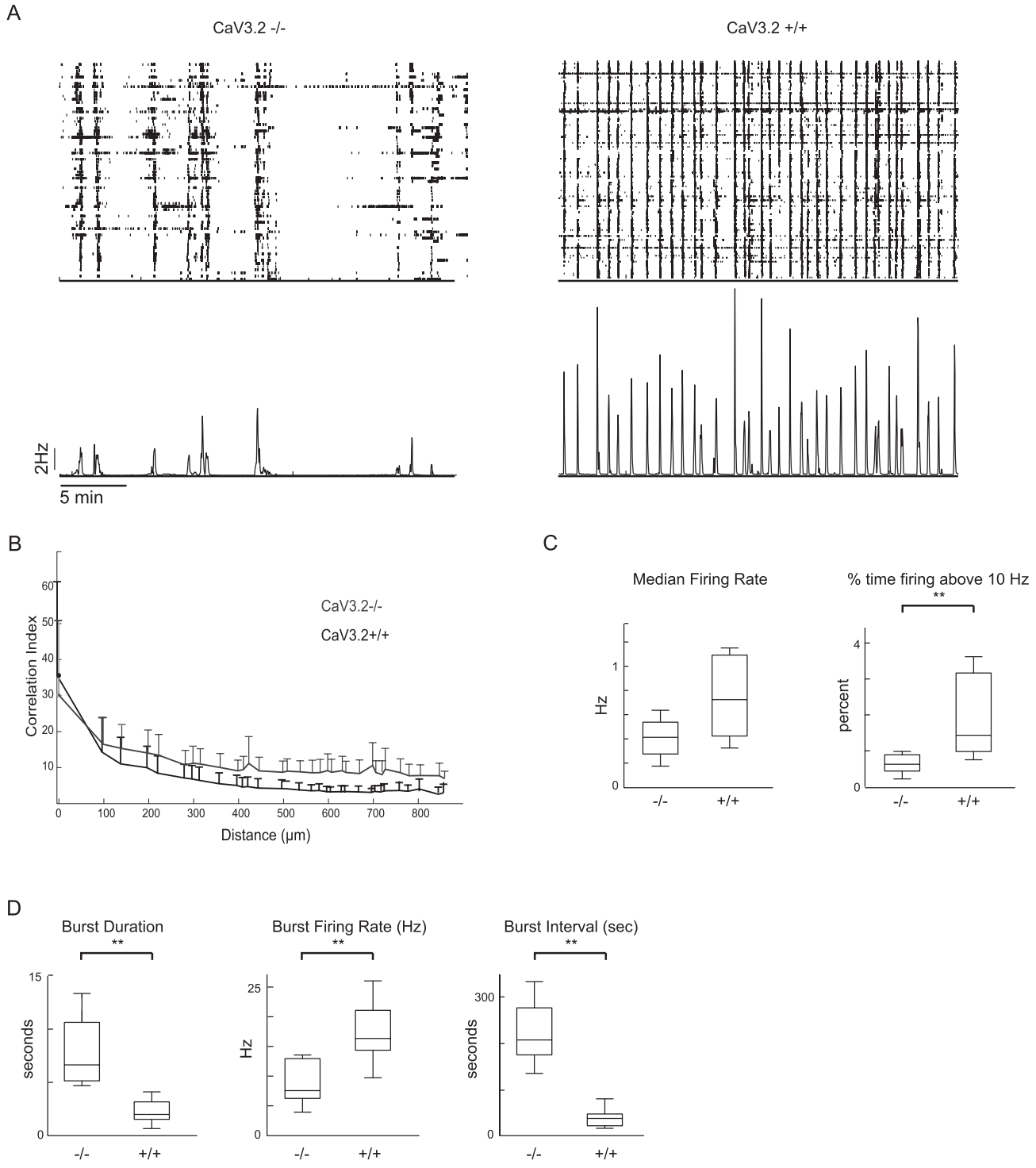



**Fig. 1.** Temporal pattern of spontaneous retinal waves is altered in CaV3.2 KO mice. (**A**) Top, Raster plot of single-unit spike trains from retinal ganglion cells recorded over a 60-minute period from P11 CaV3.2 KO (left) and CaV3.2+/+ (right) retina. Bottom, average firing rate of all units. (**B**) Pairwise correlation index as a function of intercellular distance for CaV3.2 KO (gray) and CaV3.2+/+ (black) retinas (averaged across all retinas per genotype). The data points correspond to the mean values of medians from individual datasets and the error bars represent S.E.M. The bottom error bars have been omitted for clarity. (**C/D**) Summary of the temporal properties of spontaneous firing patterns for CaV3.2 KO and CaV3.2+/+ retinas. We compute properties for all action potentials (**C**) and separately for bursts (**D**). Data are averaged over mean values for each cell of a given genotype.

the features of the bursts where we observed pronounced differences between KO and control mice (Fig. 1D). KO retinas display significantly longer burst durations (Mdn of 5.8 s; 5.11–10.53 in KO *vs*. Mdn of 2.02 s; 1.49–3.19 in control $P = 0.000502$) and interburst intervals (Mdn of 202.27 s; 170.46–270.45 in KO *vs*. Mdn of 40.91 s; 24.64–50.00 in control $P = 0.0000823$) than

https://doi.org/10.1017/S0952523814000364 Published online by Cambridge University Press

control mice. However, within the bursts, the KO firing rate is significantly lower (Mdn of 7.33 Hz; 6.04–12.83 in KO *vs*. Mdn of 16.34 Hz; 14.33–21.17 in control $P = 0.000576$). Thus, mice lacking the CaV3.2 isoform of the T-type $Ca^{2+}$ channel exhibit propagating bursts of action potentials during glutamatergic waves, but the periodicity and the properties of these spontaneous bursts are significantly altered from that of control mice.

### *CaV3.2 KO mice exhibit reduced eye-specific segregation of retinogeniculate projections*

Retinal waves drive the segregation of ipsi- and contra-lateral retinal projections into their respective anatomical layers in the dorsal lateral geniculate nucleus (dLGN) (Chan & Chiao, 2008; Elstrott et al., 2008; Guido, 2008; Huberman et al., 2008; Chen et al., 2009; Wei et al., 2011; Kirkby et al., 2013). This eye-specific segregation is disrupted when correlated firing is reduced. Therefore, we investigated whether this segregation is impacted by the prolonged, lower frequency bursts during waves in CaV3.2 KO retina.

We labeled retinogeniculate projections in KO mice and their CaV3.2+/+ littermate controls at P16 by injecting anterograde tracer cholera-toxin B into both eyes (Alexa dye conjugate, 488 left eye, 568 right eye, Fig. 2). We then compared the segregation of ipsilateral-projecting and contralateral-projecting inputs for both hemispheres of the dLGN by calculating unbiased segregation indices that quantified the degree of eye-specific segregation in the two mouse groups. Both CaV3.2 KO and controls had well-defined ipsilateral eye termination zones but the control mice showed sharper segregation (Fig. 2A). We quantified the degree of segregation as the variance of the distribution of the *R*-values for all pixels ($R = \log10 (F_I/F_C)$) with better segregated dLGNs having a wider distribution (higher variance) of the *R*-values than poorly segregated ones (Fig. 2B). We found that the degree of segregation for the KO group is significantly lower than that for the control littermates (mean ± SD of 0.3517 ± 0.0475 in KO *vs*. 0.4603 ± 0.0172 in control $n = 4$ KO and control $P = 0.0051$). Thus, the altered burst properties of CaV3.2 KO mice impact their eye-specific segregation. This highlights the important role that the bursting properties of retinal waves play in the driving activity-dependent developmental refinement of retinogeniculate projections (Sernagor et al., 2001; Butts, 2002; Tian, 2008; Blankenship & Feller, 2010; Elstrott & Feller, 2010; Xu et al., 2011).

These data indicate that (1) CaV3.2 KO mice have altered glutamatergic waves and (2) this disrupted activity pattern altered activity-dependent eye-specific refinement of retinogeniculate axons. Therefore, the CaV3.2 KO mouse offers a robust model to test the

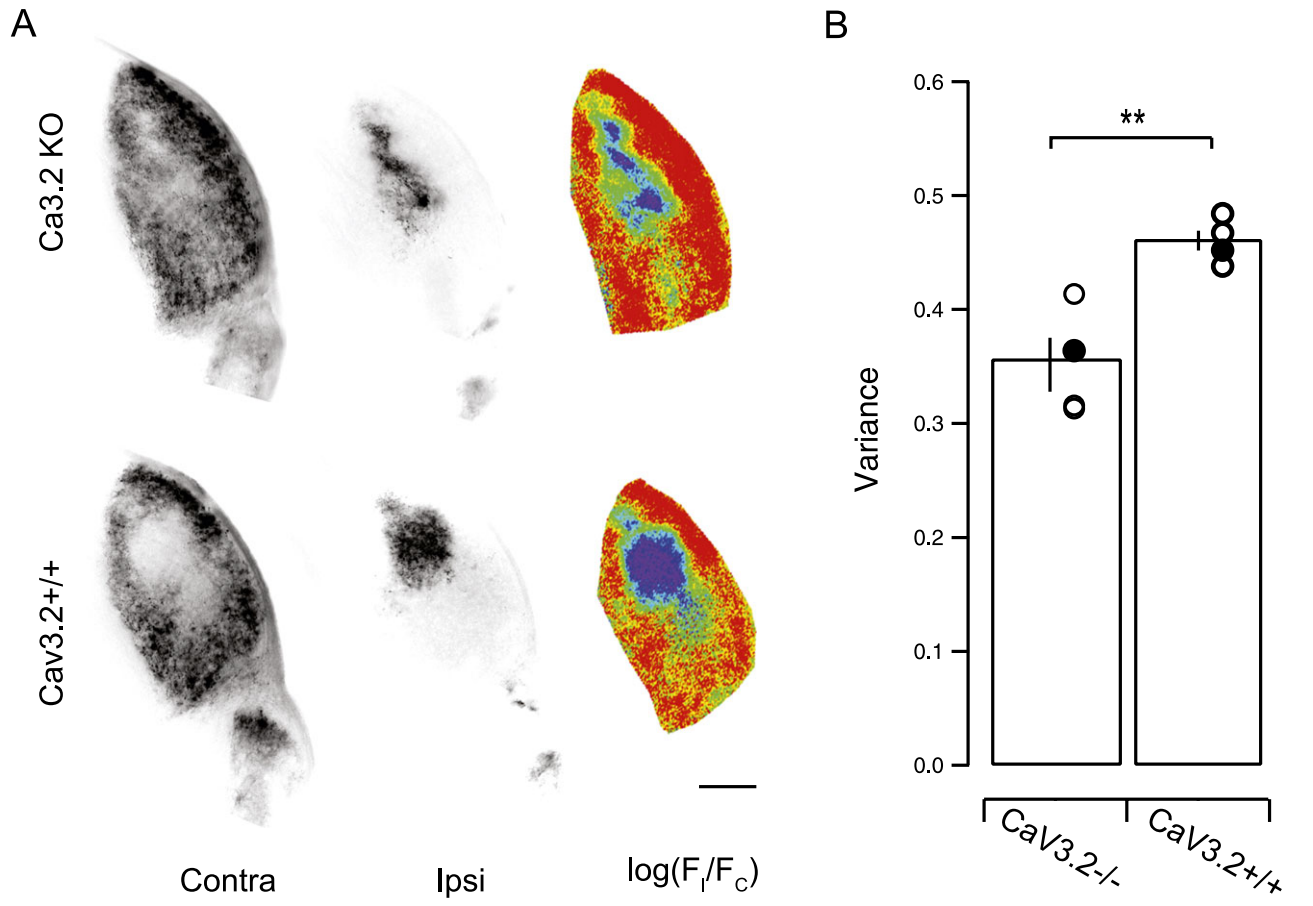



**Fig. 2.** CaV3.2 KO mice have reduced eye-specific segregation. (**A**) Fluorescence images of dLGN sections in CaV3.2 KO (top) and CaV3.2+/+ (bottom) mice. Left, fluorescence of Alexa 488-labeled, contralateral-projecting retinogeniculate axons; middle, fluorescence of Alexa 594-labeled, ipsilateral-projecting retinogeniculate axons; and right, pseudocolor images based on the logarithm of the intensity ratio ($R = \log(F_I/F_C)$) for each pixel. Scale bar, 200 $\mu$m. (**B**) Summary of the variance of the distribution of the *R*-values for all the pixels in the images of each brain. The broader the distribution of the *R*-values for a given dLGN, the greater the extent of segregation.

https://doi.org/10.1017/S0952523814000364 Published online by Cambridge University Press

contribution of various wave properties to the development of retinal direction selectivity.

### *ON–OFF DSGCs exhibit similar response properties in CaV3.2 KO and control mice*

We analyzed the direction selectivity in CaV3.2 KO mice using two approaches. First, using MEA recordings, we compared the direction selective responses of DSGCs in P16–19 CaV3.2 KO and control mice. We recorded the responses of cell populations evoked by drifting gratings, and we quantified the direction selective index (DSI) of all isolated units ($n$ = 1118 controls and 1012 KO, Fig. 3A). To selectively record from ON–OFF DSGCs, we used gratings moving at a velocity of 25 deg/s. This is above the maximum velocity for ON-DSGCs but within the tuning range for ON–OFF DSGCs (Sivyer et al., 2010). All DSGCs were confirmed to have both on and off responses (Fig. 3A, inset). Using units that have a DSI greater than 0.4 to designate them as "direction selective", we estimate that 11% of all recorded units in CaV3.2+/+ are DS (118/1012) and 13% of CaV3.2 KO (146/1118), similar to that described recently (Chen et al., 2014). These DS units were used subsequently to calculate tuning widths and firing rates. It is important to note that using MEA to calculate percentages does not necessarily accurately reflect the true representation of different cell types since the MEA itself may be selective for different subtypes of RGCs.

We compared the DSIs, firing rates, and tuning widths of ON–OFF DSGCs and found no statistically significant difference between the KO and control populations (Figs. 3B–3D). The DSI distributions of the two groups were almost identical. Both peaked near 0.0 (no tuning) and frequencies decreased uniformly as tuning approached 1.0 (perfect tuning). Notably, many ON–OFF DSGCs in both the CaV3.2 KO retina and controls had high DSIs, indicating strong tuning (DSI > 0.8). Along with similar DSI distributions, KO and control cells showed no difference in their firing rates neither for the preferred direction nor their tuning widths. Taken together, these data indicate that the altered bursting properties observed in CaV3.2 KO retinas do not affect the development of direction selectivity in ON–OFF DSGCs.

Our second approach was to use targeted cell-attached recordings from DSGCs expressing GFP in ON–OFF DSGCs. We crossed CaV3.2 KO mice with a line (TRHR-GFP) that selectively labels posterior preferring ON–OFF DSGCs (Huberman et al., 2008; Rivlin-Etzion et al., 2011), thus allowing for unambiguous targeting of a known DSGC subtype (Fig. 4). To avoid the bleaching of the photoreceptors, we identified and targeted this DSGC using two-photon targeted recordings and IR illumination (Wei et al., 2010). The overall stratification pattern of ON–OFF DSGCs was unaltered in CaV3.2 KO mice as shown by the dendritic reconstructions of filled GFP+ cells (Fig. 4A). To assay the degree of directional tuning, we used cell-attached recordings to determine the action potential generated in response to drifting gratings (Fig. 4B). Most cells recorded from KO animals ($n$ = 7/10) display sharp directional tuning (DSI > 0.4) and a clear ON/OFF response to flashing spots (data not shown) with no significant difference in the average DSI (Fig. 4C). These data confirm that for an identified subtype of ON–OFF DSGCs, the emergence

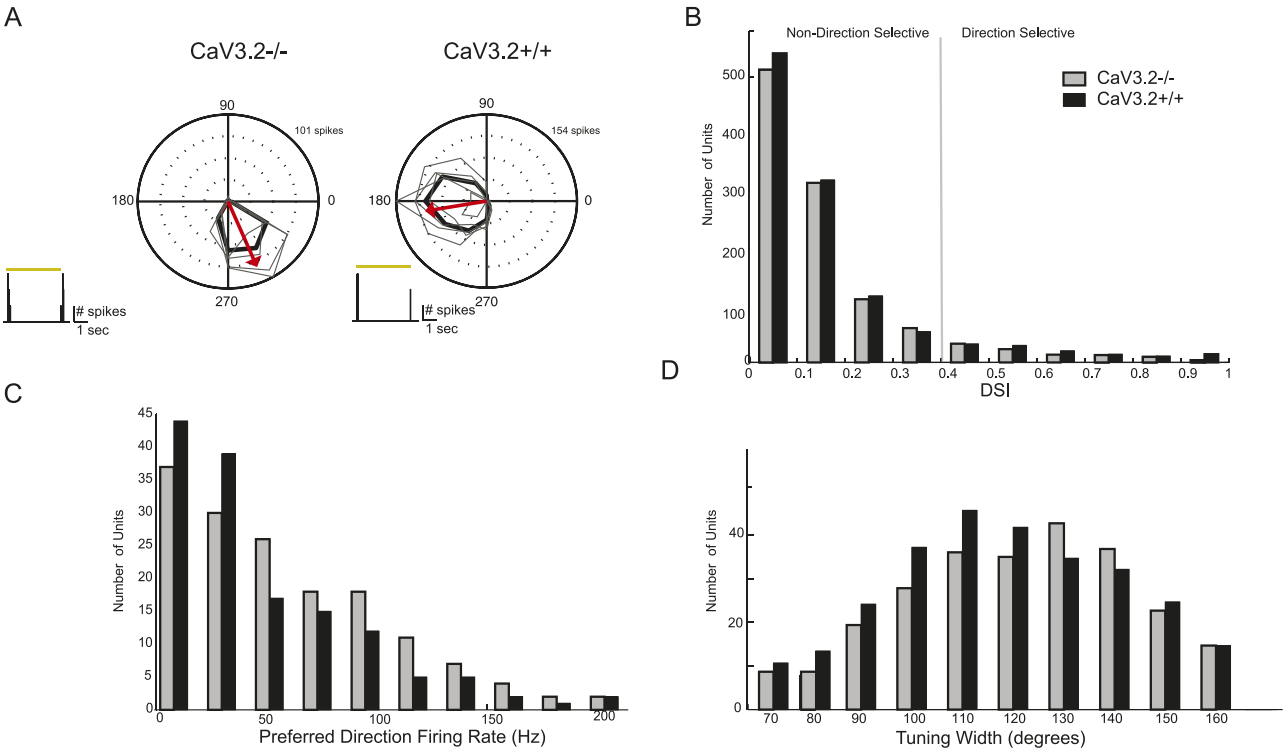



**Fig. 3.** CaV3.2 KO mice have distribution of directional responses that are indistinguishable from control. (**A**) Polar plot of mean spike rate response to motion in 12 directions across five repetitions from CaV3.2 KO and CaV3.2+/+ retinas. The tuning curve was obtained using the mean firing rate in response to each direction. The arrow indicates mean preferred direction of the example cell. (**B**) Summary of the distribution for DSI from all CaV3.2 KO and CaV3.2+/+ units. (**C**) Summary of the distribution for maximum firing rate in the preferred direction. (**D**) Summary of the distribution of tuning widths as based on fitting tuning curves to a von Mises distribution (see Materials and methods).

https://doi.org/10.1017/S0952523814000364 Published online by Cambridge University Press

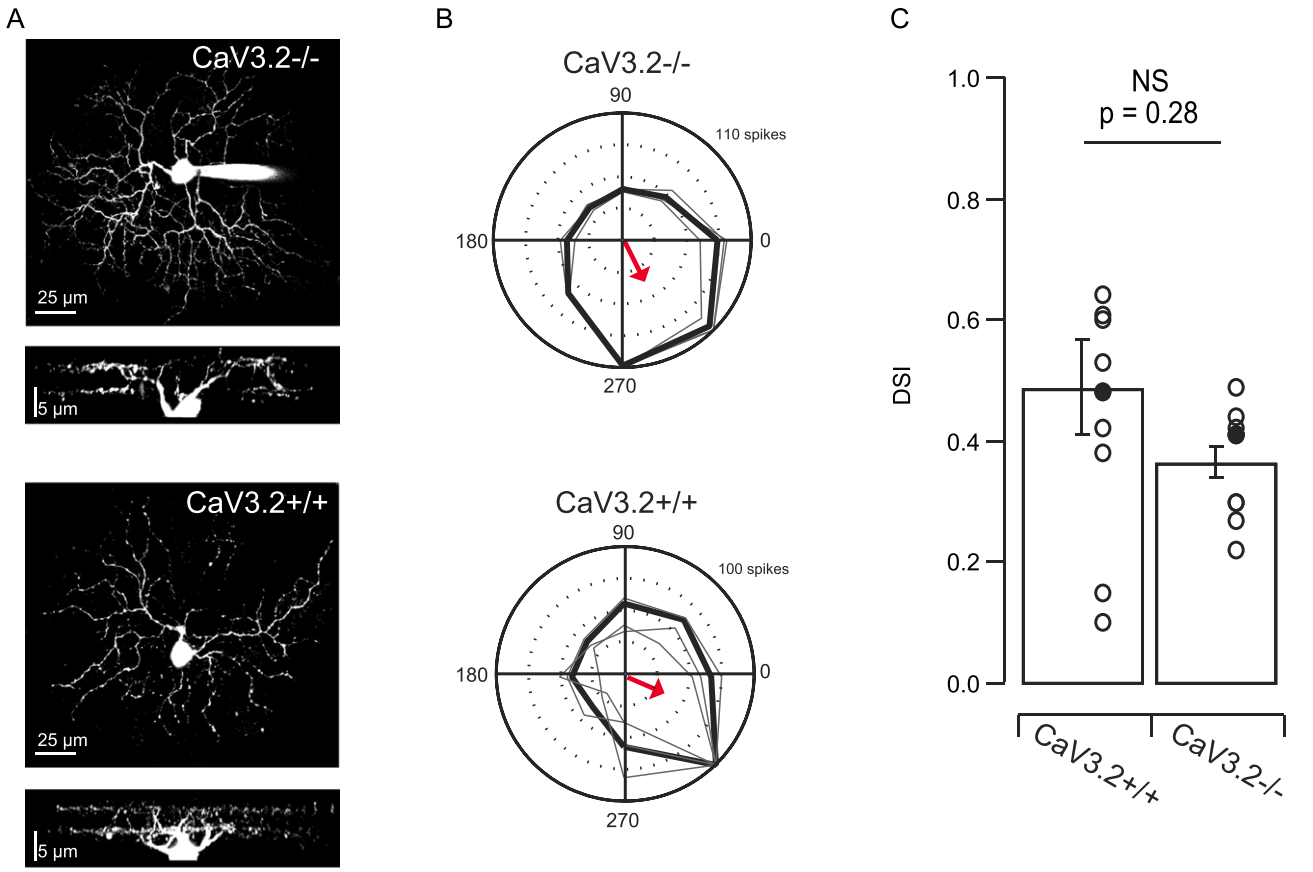



**Fig. 4.** Targeted cell-attached recordings from identified ON–OFF DSGCs have similar tuning in CaV3.2 KO and CaV3.2+/+ mice. (**A**) Maximal intensity projections of *z*-stack images of two ON–OFF DSGCs (filled with Alexa Fluor 488) and side views of the complete dendritic arborizations showing dendritic arbors in the on and off sublaminae from CaV3.2–/– and CaV3.2+/+ mouse. (**B**) Targeted two-photon recordings of light responses from GFP+ cells in transgenic mice in which GFP is expressed in subtype of DSGCs. Polar plots of mean spike rate response to motion in eight directions across three repetitions from CaV3.2–/– (top) and CaV3.2+/+ (bottom) retinas. The tuning curve was obtained using the mean firing rate in response to each direction. The radius scale is the normalization of the spike-count in each direction. The maximum response is the spike-count in the preferred direction, and it is written in the top right corner of the polar plots. The arrow indicates mean preferred direction of the example cell. (**C**) Summary data comparing DSIs in CaV3.2+/+ and CaV3.2–/–.

of mature direction selective responses is not affected by the changes in spontaneous activity in CaV3.2 KO mice.

## Discussion

We have identified a genetic model for studying the effects of altered waves on the development of retinal circuits. CaV3.2 KO retinas display normal spatial correlations during waves but their cells exhibited altered bursting properties with longer interburst intervals, prolonged burst durations, and lower burst firing rates. These changes disrupted eye-specific segregation of the retinogeniculate afferents. However, in both transgenically labeled posterior preferring ON–OFF DSGCs and whole retinal populations, these changes did not detectably affect the direction selective responses. Therefore, the precise pattern of high-frequency burst activity provided by glutamatergic retinal waves does not seem to play a role in the development of retinal direction selectivity.

The idea that retinal waves are involved in the development of direction selectivity is supported by three compelling observations. First, several cell types in the circuit that mediates retinal waves—including bipolar cells, starburst amacrine cells, and DSGCs—are depolarized during these waves (Zhou, 1998; Elstrott & Feller, 2010; Ford et al., 2012; Akrouh & Kerschensteiner, 2013; Firl et al., 2013). Thus, they are robustly activated by spontaneous activity. Hence, these waves could act potentially as a proxy for moving visual stimuli that activate directional circuits. Second, the retinal waves exhibit a noticeable bias in their direction of wave propagation, with more waves traveling along the nasal axis than along the other three cardinal axes (Stafford et al., 2009; Elstrott & Feller, 2010). Hence, the firing patterns induced by these waves contain information about the cardinal coordinates of the retina by encoding the nasal direction. Third, blocking synaptic release from bipolar cells during the second postnatal week reduces the rate of synapse formation leading to weaker connections between bipolar and ganglion cells (Ma & Pan, 2003; Kerschensteiner et al., 2009). Hence, the retinal waves may provide a source of depolarization that is necessary for preserving the appropriate synapses and/or for pruning the inappropriate synapses in order to properly wire up directional circuits.

That direction selectivity develops independent of retinal waves also has support. First, though DSGCs are depolarized by the nasally biased retinal waves, their spiking is not influenced by this bias. In other words, nasal-preferring DSGCs fire the same number of action potentials regardless of the wave's direction of

https://doi.org/10.1017/S0952523814000364 Published online by Cambridge University Press

motion (Elstrott & Feller, 2010), indicating that waves do not evoke the same responses in DSGCs that moving visual stimuli do. Second, pharmacological manipulations during the second postnatal week do not prevent the detection of DSGCs. For example, intraocular injections of muscimol, a GABA-A receptor agonist that silences neuronal firing (Wei et al., 2011), do not prevent the development of the directional selective responses. Similarly, intraocular injections of GABA-A receptor antagonists (Sun et al., 2011; Wei et al., 2011) blocking the inhibitory circuits mediating direction selectivity, and tetrodotoxin (TTX) (Sun et al., 2011) preventing DSGC spiking activity also do not prevent the development of direction selectivity. However, as noted earlier, *in vivo* assessments of the effect of intraocular injections are difficult, though in one study, the vitreous humor from retinas that had received repeated pharmacological injections for TTX and nicotinic acetylcholine receptor antagonists blocked retinal waves *in vitro* (Sun et al., 2011). It is important to note that excluding a role for postsynaptic spiking with TTX does not rule out a role for patterned presynaptic synaptic activity to play a role in activity-dependent plasticity as observed in visual cortex (e.g., Frenkel & Bear, 2004; Turrigiano & Nelson, 2004). Third, DSGCs have been detected as early as P11 in mouse retina (Chen et al., 2009; Yonehara et al., 2011) indicating that the circuits are established prior to glutamatergic retinal waves. As noted by these studies (Fig. 3) and others (Chan & Chiao, 2008; Elstrott & Feller, 2010; Rivlin-Etzion et al., 2011; Chen et al., 2014), the distribution of DSIs is very broad across the population. Hence, finding the examples of DSGCs at P11 does not mean all subtypes of DSGCs and even all preferred directions have developed normally.

We approached the role of retinal waves in the development of direction selectivity in a different way. We sought to identify and investigate genetic models in which waves are selectively altered or diminished without affecting the direction-selective circuit itself. This is particularly challenging for glutamate-receptor mediated waves because the manipulation needs to affect the wave-generating mechanism but not the light response, and both of these mechanisms rely upon the activation of ionotropic glutamate receptors (Blankenship & Feller, 2010). One such model was recently described (Xu et al., 2011), but the effect on DSGCs has yet to be explored.

We found that in CaV3.2 KO mice, the pattern of glutamatergic waves was significantly altered, in that they occurred much less frequently and that the bursts associated with waves were longer in duration with a lower firing rate. Glutamatergic waves are mediated by glutamate release from bipolar cells (Akrouh & Kerschensteiner, 2013; Firl et al., 2013), however, which aspects of the circuit control burst properties and the frequency of waves are not yet identified. In the retina, the T-type channels have been described in bipolar cell terminals and RGCs (Pan et al., 2001; Lee et al., 2003; Ma & Pan, 2003; Hu et al., 2009; Cui et al., 2012; Sargoy et al., 2014). Hence, future experiments will be necessary to determine whether these changes are due to changes in the pacemaking or release properties from bipolar cells or in the excitability of RGCs.

While it does not appear that the spontaneous activity plays a role in the development of direction selectivity in the retina, there may still be a more general role for visually evoked activity in the maturation of the distinct cardinal grouping of DSGC subtypes in the mature retina. A recent study demonstrated that at eye-opening in both rabbit and mouse, the distribution of preferred directions was uniformly distributed, rather than showing segregation along the four cardinal axes, indicating that a process of refinement in the preferred direction occurs after eye-opening (Chan & Chiao, 2013). They also found a slight degree of anisotropy in the distribution of preferred directions in dark reared animals. In addition, an improvement of DSGC tuning was observed after eye-opening (Chen et al., 2014). Together, these findings suggest that the process of establishing strong null-side inhibition that underlies direction selectivity may differ from the mechanism that ultimately determines functional preferred direction in DSGCs and that activity may play a role in the latter.

In summary, this study demonstrates that the CaV3.2 subunit of the T-type $Ca^{2+}$ channel is important for shaping bursting activity that occurs during retinal waves. Although the circuit that underlies direction selectivity coincidently undergoes a period of critical synaptic maturation during this time, introducing a persistent and dramatic alteration in the activity present during the second postnatal week did not affect the development of the robust directional responses after eye-opening. These results and others indicate that the final stages of development in the direction selective circuit in the retina do not require spontaneous activity.

## Acknowledgments

This work was supported by NIH Grants R01EY019498, R01EY013528, and P30EY003176 (MBF) and NIH Grant 5F31NS071784 (AMH). We thank Dr. Lowry Kirkby and Dr. Alana Firl for help with analysis of MEA recordings.

## References

Akrouh, A. & Kerschensteiner, D. (2013). Intersecting circuits generate precisely patterned retinal waves. *Neuron* **79**, 322–334.

Barlow, H.B. & Hill, R.M. (1963). Selective sensitivity to direction of movement in ganglion cells of the rabbit retina. *Science* **139**, 412–414.

Blankenship, A.G. & Feller, M.B. (2010). Mechanisms underlying spontaneous patterned activity in developing neural circuits. *Nature Reviews Neuroscience* **11**, 18–29.

Blankenship, A.G., Hamby, A.M., Firl, A., Vyas, S., Maxeiner, S., Willecke, K. & Feller, M.B. (2011). The role of neuronal connexins 36 and 45 in shaping spontaneous firing patterns in the developing retina. *The Journal of Neuroscience* **31**, 9998–10008.

Borst, A. & Euler, T. (2011). Seeing things in motion: Models, circuits, and mechanisms. *Neuron* **71**, 974–994.

Butts, D.A. (2002). Retinal waves: Implications for synaptic learning rules during development. *Neuroscientist* **8**, 243–253.

Cain, S.M. & Snutch, T.P. (2013). T-type calcium channels in burst-firing, network synchrony, and epilepsy. *Biochimica et Biophysica Acta* **1828**, 1572–1578.

Chan, Y-C. & Chiao, C-C. (2008). Effect of visual experience on the maturation of ON-OFF direction selective ganglion cells in the rabbit retina. *Vision Research* **48**, 2466–2475.

Chan, Y-C. & Chiao, C-C. (2013). The distribution of the preferred directions of the ON-OFF direction selective ganglion cells in the rabbit retina requires refinement after eye opening. *Physiological Reports* **1**, e00013.

Chen, C-C., Lamping, K.G., Nuno, D.W., Barresi, R., Prouty, S.J., Lavoie, J.L., Cribbs, L.L., England, S.K., Sigmund, C.D., Weiss, R.M., Williamson, R.A., Hill, J.A. & Campbell, K.P. (2003). Abnormal coronary function in mice deficient in alpha1H T-type Ca2+ channels. *Science* **302**, 1416–1418.

Chen, H., Liu, X. & Tian, N. (2014). Subtype-dependent postnatal development of direction- and orientation-selective retinal ganglion cells in mice. *Journal of Neurophysiology* **112**, 2092–2101.

Chen, M., Weng, S., Deng, Q., Xu, Z. & He, S. (2009). Physiological properties of direction-selective ganglion cells in early postnatal and adult mouse retina. *The Journal of Physiology* **587**, 819–828.

Cueni, L., Canepari, M., Adelman, J.P. & Lüthi, A. (2009). Ca(2+) signaling by T-type Ca(2+) channels in neurons. *Pflugers Archiv: European Journal of Physiology* **457**, 1161–1172.

Cui, J., Ivanova, E., Qi, L. & Pan, Z.H. (2012). Expression of CaV3.2 T-type $Ca^{2+}$ channels in a subpopulation of retinal type-3 cone bipolar cells. *Neuroscience* **224**, 63–69.

https://doi.org/10.1017/S0952523814000364 Published online by Cambridge University Press

Elstrott, J. & Feller, M.B. (2010). Direction-selective ganglion cells show symmetric participation in retinal waves during development. *The Journal of Neuroscience* **30**, 11197–11201.

Elstrott, J., Anishchenko, A., Greschner, M., Sher, A., Litke, A.M., Chichilnisky, E.J. & Feller, M.B. (2008). Direction selectivity in the retina is established independent of visual experience and cholinergic retinal waves. *Neuron* **58**, 499–506.

Firl, A., Sack, G.S., Newman, Z.L., Tani, H. & Feller, M.B. (2013). Extrasynaptic glutamate and inhibitory neurotransmission modulate ganglion cell participation during glutamatergic retinal waves. *Journal of Neurophysiology* **109**, 1969–1978.

Ford, K.J. & Feller, M.B. (2012). Assembly and disassembly of a retinal cholinergic network. *Visual Neuroscience* **29**, 61–71.

Ford, K.J., Félix, A.L. & Feller, M.B. (2012). Cellular mechanisms underlying spatiotemporal features of cholinergic retinal waves. *The Journal of Neuroscience* **32**, 850–863.

Frenkel, M.Y. & Bear, M.F. (2004). How monocular deprivation shifts ocular dominance in visual cortex of young mice. *Neuron* **44**, 917–923.

Galli, L. & Maffei, L. (1988). Spontaneous impulse activity of rat retinal ganglion cells in prenatal life. *Science* **242**, 90–91.

Guido, W. (2008). Refinement of the retinogeniculate pathway. *The Journal of Physiology* **586**, 4357–4362.

Hu, C., Bi, A. & Pan, Z-H. (2009). Differential expression of three T-type calcium channels in retinal bipolar cells in rats. *Visual Neuroscience* **26**, 177–187.

Huberman, A.D., Feller, M.B. & Chapman, B. (2008). Mechanisms underlying development of visual maps and receptive fields. *Annual Review of Neuroscience* **31**, 479–509.

Huberman, A.D., Wei, W., Elstrott, J., Stafford, B.K., Feller, M.B. & Barres, B.A. (2009). Genetic identification of an On-Off direction-selective retinal ganglion cell subtype reveals a layer-specific subcortical map of posterior motion. *Neuron* **62**, 327–334.

Kay, J.N., De la Huerta, I., Kim, I.J., Zhang, Y., Yamagata, M., Chu, M.W., Meister, M. & Sanes, J.R. (2011). Retinal ganglion cells with distinct directional preferences differ in molecular identity, structure, and central projections. *The Journal of Neuroscience* **31**, 7753–7762.

Kerschensteiner, D., Morgan, J.L., Parker, E.D., Lewis, R.M. & Wong, R.O.L. (2009). Neurotransmission selectively regulates synapse formation in parallel circuits in vivo. *Nature* **460**, 1016–1020.

Kirkby, L.A., Sack, G.S., Firl, A. & Feller, M.B. (2013). A role for correlated spontaneous activity in the assembly of neural circuits. *Neuron* **80**, 1129–1144.

Lee, S.C., Hayashida, Y. & Ishida, A.T. (2003). Availability of low-threshold Ca2+ current in retinal ganglion cells. *Journal of Neurophysiology* **90**, 3888–3901.

Ma, Y.P. & Pan, Z.H. (2003). Spontaneous regenerative activity in mammalian retinal bipolar cells: Roles of multiple subtypes of voltage-dependent Ca2+ channels. *Visual Neuroscience* **20**, 131–139.

Maccione, A., Hennig, M.H., Gandolfo, M., Muthmann, O., van Coppenhagen, J., Eglen, S.J., Berdondini, L. & Sernagor, E. (2014). Following the ontogeny of retinal waves: Pan-retinal recordings of population dynamics in the neonatal mouse. *The Journal of Physiology* **592**, 1545–1563.

Marshel, J.H., Kaye, A.P., Nauhaus, I. & Callaway, E.M. (2012). Anterior-posterior direction opponency in the superficial mouse lateral geniculate nucleus. *Neuron* **76**, 713–720.

Meister, M., Wong, R.O., Baylor, D.A. & Shatz, C.J. (1991). Synchronous bursts of action potentials in ganglion cells of the developing mammalian retina. *Science* **252**, 939–943.

Pan, Z.H., Hu, H.J., Perring, P. & Andrade, R. (2001). T-type Ca(2+) channels mediate neurotransmitter release in retinal bipolar cells. *Neuron* **32**, 89–98.

Perez-Reyes, E. (2003). Molecular physiology of low-voltage-activated t-type calcium channels. *Physiological Reviews* **83**, 117–161.

Piscopo, D.M., El-Danaf, R.N., Huberman, A.D. & Niell, C.M. (2013). Diverse visual features encoded in mouse lateral geniculate nucleus. *The Journal of Neuroscience* **33**, 4642–4656.

Puthussery, T., Percival, K.A., Venkataramani, S., Gayet-Primo, J., Grünert, U. & Taylor, W.R. (2014). Kainate receptors mediate synaptic input to transient and sustained OFF visual pathways in primate retina. *The Journal of Neuroscience* **34**, 7611–7621.

Rivlin-Etzion, M., Zhou, K., Wei, W., Elstrott, J., Nguyen, P.L., Barres, B.A., Huberman, A.D. & Feller, M.B. (2011). Transgenic mice reveal unexpected diversity of on-off direction-selective retinal ganglion cell subtypes and brain structures involved in motion processing. *The Journal of Neuroscience* **31**, 8760–8769.

Sargoy, A., Sun, X., Barnes, S. & Brecha, N.C. (2014). Differential calcium signaling mediated by voltage-gated calcium channels in rat retinal ganglion cells and their unmyelinated axons. *PLoS ONE* **9**, e84507.

Sernagor, E., Eglen, S.J. & Wong, R.O. (2001). Development of retinal ganglion cell structure and function. *Progress in Retinal and Eye Research* **20**, 139–174.

Singer, J.H. & Diamond, J.S. (2003). Sustained Ca2+ entry elicits transient postsynaptic currents at a retinal ribbon synapse. *The Journal of Neuroscience* **23**, 10923–10933.

Sivyer, B., van Wyk, M., Vaney, D.I. & Taylor, W.R. (2010). Synaptic inputs and timing underlying the velocity tuning of direction-selective ganglion cells in rabbit retina. *The Journal of Physiology* **588**, 3243–3253.

Stafford, B.K., Sher, A., Litke, A.M. & Feldheim, D.A. (2009). Spatial-temporal patterns of retinal waves underlying activity-dependent refinement of retinofugal projections. *Neuron* **64**, 200.

Sun, L., Han, X. & He, S. (2011). Direction-selective circuitry in rat retina develops independently of GABAergic, cholinergic and action potential activity. *PLoS ONE* **6**, e19477.

Tian, N. (2008). Synaptic activity, visual experience and the maturation of retinal synaptic circuitry. *The Journal of Physiology* **586**, 4347–4355.

Torborg, C.L. & Feller, M.B. (2004). Unbiased analysis of bulk axonal segregation patterns. *Journal of Neuroscience Methods* **135**, 17–26.

Torborg, C.L., Hansen, K.A. & Feller, M.B. (2005). High frequency, synchronized bursting drives eye-specific segregation of retinogeniculate projections. *Nature Neuroscience* **8**, 72–78 Epub2004Dec19.

Turrigiano, G.G. & Nelson, S.B. (2004). Homeostatic plasticity in the developing nervous system. *Nature Reviews Neuroscience* **5**, 97–107.

Wei, W. & Feller, M.B. (2011). Organization and development of direction-selective circuits in the retina. *Trends in Neurosciences* **34**, 638–645.

Wei, W., Elstrott, J. & Feller, M.B. (2010). Two-photon targeted recording of GFP-expressing neurons for light responses and live-cell imaging in the mouse retina. *Nature Protocols* **5**, 1347–1352.

Wei, W., Hamby, A.M., Zhou, K. & Feller, M.B. (2011). Development of asymmetric inhibition underlying direction selectivity in the retina. *Nature* **469**, 402–406 Epub2010Dec5.

Wong, R.O.L. (1999). Retinal waves and visual system development. *Annual Review of Neuroscience* **22**, 29–47.

Xu, H-P., Chen, H., Ding, Q., Xie, Z-H., Chen, L., Diao, L., Wang, P., Gan, L., Crair, M.C. & Tian, N. (2010). The immune protein CD3zeta is required for normal development of neural circuits in the retina. *Neuron* **65**, 503–515.

Xu, H.P., Furman, M., Mineur, Y.S., Chen, H., King, S.L., Zenisek, D., Zhou, Z.J., Butts, D.A., Tian, N., Picciotto, M.R. & Crair, M.C. (2011). An instructive role for patterned spontaneous retinal activity in mouse visual map development. *Neuron* **70**, 1115–1127.

Yonehara, K., Balint, K., Noda, M., Nagel, G., Bamberg, E. & Roska, B. (2011). Spatially asymmetric reorganization of inhibition establishes a motion-sensitive circuit. *Nature* **469**, 407–410.

Zhou, Z.J. (1998). Direct participation of starburst amacrine cells in spontaneous rhythmic activities in the developing mammalian retina. *The Journal of Neuroscience* **18**, 4155–4165.

https://doi.org/10.1017/S0952523814000364 Published online by Cambridge University Press